

TRIP8b Splice Forms Act in Concert to Regulate the Localization and Expression of HCN1 Channels in CA1 Pyramidal Neurons

Rebecca Piskorowski,¹ Bina Santoro,¹ and Steven A. Siegelbaum^{1,2,3,*}

¹Department of Neuroscience

²Department of Pharmacology

³Howard Hughes Medical Institute

Columbia University, 1051 Riverside Drive, New York, NY 10032, USA

*Correspondence: sas8@columbia.edu

DOI 10.1016/j.neuron.2011.03.023

SUMMARY

HCN1 channel subunits, which contribute to the hyperpolarization-activated cation current (I_h), are selectively targeted to distal apical dendrites of hippocampal CA1 pyramidal neurons. Here, we addressed the importance of the brain-specific auxiliary subunit of HCN1, TRIP8b, in regulating HCN1 expression and localization. More than ten N-terminal splice variants of TRIP8b exist in brain and exert distinct effects on HCN1 trafficking when overexpressed. We found that isoform-wide disruption of the TRIP8b/HCN1 interaction caused HCN1 to be mistargeted throughout CA1 somatodendritic compartments. In contrast, HCN1 was targeted normally to CA1 distal dendrites in a TRIP8b knockout mouse that selectively lacked exons 1b and 2. Of the two remaining hippocampal TRIP8b isoforms, TRIP8b(1a-4) promoted HCN1 surface expression in dendrites, whereas TRIP8b(1a) suppressed HCN1 misexpression in axons. Thus, proper subcellular localization of HCN1 depends on its differential additive and subtractive sculpting by two isoforms of a single auxiliary subunit.

INTRODUCTION

Ion channels are often targeted to select regions of a neuron where they locally regulate specific physiological functions. HCN1 channels, which generate the hyperpolarization-activated cation current, I_h, are expressed in the apical dendrites of hippocampal CA1 pyramidal neurons in a striking gradient of increasing density with increasing distance from the soma (Lorincz et al., 2002; Magee, 1998; Notomi and Shigemoto, 2004; Santoro et al., 1997). As a consequence, I_h acts as a relatively selective inhibitory constraint of the direct cortical perforant path (PP) inputs to CA1 neurons, which terminate on CA1 distal dendrites in *stratum lacunosum moleculare* (SLM) (Nolan et al., 2004; Tsay et al., 2007). In contrast, HCN1 has less effect

at Schaffer collateral (SC) synapses, which arise from hippocampal CA3 neurons and terminate on more proximal CA1 dendrites in *stratum radiatum* (SR). Thus, trafficking of HCN1 to distal dendrites selectively constrains the cortical versus hippocampal inputs to CA1 neurons, which may contribute to the effect of HCN1 to constrain spatial learning and memory (Nolan et al., 2004).

Despite the importance of the subcellular targeting of HCN1, the molecular mechanisms underlying this regulatory control remain unknown. One promising candidate is the auxiliary subunit of HCN channels TRIP8b (Santoro et al., 2004). This brain-specific cytoplasmic protein binds to all HCN channels (HCN1-4) and regulates HCN gating in both heterologous expression systems and hippocampal cultures (Lewis et al., 2009; Santoro et al., 2009; Zolles et al., 2009). TRIP8b undergoes extensive alternative splicing at its N terminus, with more than ten isoforms expressed in brain. There are two alternate translation start sites (exons 1a or 1b) followed by variable combinations of exons 2, 3, and 4. The majority of the protein, encoded by exons 5–16, is constant among isoforms. The various TRIP8b isoforms exert dramatically different effects to upregulate or downregulate HCN1 surface expression when overexpressed heterologously or in dissociated neurons.

Based on real-time PCR and western blot analysis of brain tissue, TRIP8b(1a-4), and TRIP8b(1a) represent the two most prominently expressed isoforms, with TRIP8b(1b-2) expressed at somewhat lower levels (Lewis et al., 2009; Santoro et al., 2004, 2009). TRIP8b(1b-2) overexpression causes a near complete loss of HCN1 surface expression and I_h, in both heterologous cells and hippocampal neurons (Lewis et al., 2009; Santoro et al., 2004, 2009). This effect is likely caused by clathrin-mediated channel endocytosis through the binding of adaptor protein (AP) complexes to specific tyrosine-based and dileucine trafficking motifs in the TRIP8b N terminus (Santoro et al., 2004, 2009). In contrast, TRIP8b(1a-4) enhances surface expression of HCN1 (Lewis et al., 2009; Santoro et al., 2009). The effect of TRIP8b(1a) depends on cellular context, causing a 10-fold decrease in HCN1 surface expression in oocytes (Santoro et al., 2009, 2011) while enhancing HCN1 expression in HEK293 cells (Lewis et al., 2009).

Although exogenously expressed TRIP8b is a potent regulator of HCN1 in vitro and in vivo, little is known about how

endogenous TRIP8b controls HCN1 trafficking in the brain. Using immunohistochemical, electrophysiological, and genetic targeting approaches, we found that endogenous TRIP8b is a necessary element for the trafficking of HCN1 to the surface membrane of CA1 pyramidal cells in vivo. Moreover, we found that TRIP8b(1a-4), which upregulates HCN1 in heterologous systems, is the key isoform involved in dendritic expression of HCN1. In contrast, TRIP8b(1a), which causes downregulation of HCN1 surface expression in *Xenopus* oocytes, is important for preventing mislocalization of HCN1 in the axons of CA1 pyramidal neurons. Furthermore, we provide evidence that TRIP8b isoforms containing exon 1b are largely expressed in oligodendrocytes, where they are coexpressed with HCN2 (Notomi and Shigemoto, 2004). Thus, the variety of TRIP8b N-terminal splice isoforms is important for differential regulation of HCN channels in distinct neuronal compartments and distinct cell types.

RESULTS

TRIP8b Knockdown Reduces Ih in CA1 Pyramidal Neurons Both In Vitro and In Vivo

To investigate the role of TRIP8b in the regulation of HCN1 channels in vivo, we reduced endogenous levels of all isoforms using short interfering RNA (siRNA) designed against a constant region of TRIP8b. A lentivirus vector delivered either the TRIP8b-specific siRNA or a scrambled control siRNA. The same vector also independently expressed enhanced green fluorescent protein (EGFP) to mark infected neurons. We confirmed the efficacy and specificity of our chosen siRNA sequence in dissociated hippocampal neuron cultures (Figures 1A–1D). TRIP8b siRNA reduced the amount of TRIP8b protein in western blots relative to control siRNA. Furthermore, the amplitude of Ih in whole-cell voltage-clamp recordings was significantly smaller in neurons expressing TRIP8b siRNA versus neurons expressing control siRNA. Thus, Ih density (see Supplemental Experimental Procedures available online) was reduced from 1.40 ± 0.2 pA/pF (mean \pm SEM, $N = 21$ cells) in neurons infected with control siRNA to 0.35 ± 0.05 pA/pF ($N = 23$ cells) in neurons infected with TRIP8b siRNA ($p < 0.01$, t test). These results confirm those of Lewis et al. (2009), who used a different siRNA sequence to knockdown TRIP8b in vitro. In independent experiments, we verified that both TRIP8b siRNAs exerted similar effects to reduce Ih amplitude (R.P. and S.A.S., unpublished data). When we measured whole cell currents in the presence of the Ih antagonist ZD7288 (10 μ M), there was no difference in current amplitude from cells expressing TRIP8b siRNA versus control siRNA (Figure 1B; current density was 0.22 ± 0.03 pA/pF with control siRNA and 0.18 ± 0.02 pA/pF with TRIP8b siRNA; $p > 0.5$, t test). This provides strong evidence that the action of TRIP8b siRNA is specific for Ih with no obvious off-target effects.

As HCN1 is not properly targeted to distal dendrites of hippocampal neurons in dissociated cell cultures, we examined the effect of reducing TRIP8b levels on Ih expression in CA1 pyramidal neurons in vivo. Lentivirus encoding TRIP8b siRNA or control siRNA was injected under stereotactic control into the CA1 region of the hippocampus of 5-week-old mice. After 2 weeks, brains were dissected and sliced for immunohisto-

chemical analysis. The EGFP-positive (infected) regions of CA1 from hippocampi expressing TRIP8b siRNA had reduced levels of TRIP8b staining compared with neighboring regions of CA1 that were not EGFP-positive (Figure S1). No change in TRIP8b staining was detected in slices infected with virus expressing control siRNA, confirming the in vivo efficacy and specificity of the siRNA.

To examine the effect of in vivo knockdown of TRIP8b on HCN channel surface density, we obtained whole-cell recordings from EGFP-positive CA1 pyramidal neurons in acute slices from hippocampi injected with virus expressing either TRIP8b siRNA or control siRNA. Because of limitations in achieving adequate voltage-clamp of CA1 dendrites in acute slices, we relied on current clamp measurements of electrophysiological parameters known to reflect Ih (Magee, 1998, 1999) and HCN1 (Nolan et al., 2004). We found that CA1 neurons infected with TRIP8b siRNA displayed a series of changes consistent with a marked reduction in Ih. First, there was a ~ 3 mV negative shift in the resting potential of neurons infected with TRIP8b siRNA (-72.1 ± 1.0 mV; $n = 15$) compared with control siRNA (-69.0 ± 0.9 mV; $n = 18$; $p < 0.05$, t test), consistent with a loss of the depolarizing influence of Ih. Moreover, this difference was eliminated in the presence of ZD7288 (TRIP8b siRNA: -78.7 ± 0.9 mV; $n = 15$; control siRNA: -78.4 ± 0.7 mV; $n = 18$), indicating a specific role of Ih (Figure 1B). Second, knockdown of TRIP8b caused a large increase in input resistance (TRIP8b siRNA: 140.5 ± 9.9 M Ω ; $n = 15$; control siRNA: 89.67 ± 5.1 M Ω ; $n = 18$; $p < 0.01$, t test), consistent with the loss of HCN channels (Figure 1F). This effect was also abolished by ZD7288 (TRIP8b siRNA: 189.9 ± 11.4 M Ω ; $n = 15$; control: 180.1 ± 10.5 M Ω ; $n = 18$). Third, the depolarizing sag in response to a hyperpolarizing current step, characteristic of Ih activation, was significantly decreased in CA1 neurons infected with TRIP8b siRNA (TRIP8b siRNA: sag ratio = 0.10 ± 0.02 ; $n = 15$; control: sag ratio = 0.24 ± 0.02 ; $n = 18$; $p < 0.01$, t test) (Figure 1G). In neurons expressing TRIP8b or control siRNA, the sag was eliminated by 10 μ M ZD7288.

Next, we examined changes in Ih based on the decay time course of the PP EPSP, which is sped up by HCN channels in distal dendrites (Magee, 1999; Nolan et al., 2004). Knockdown of TRIP8b led to a $\sim 70\%$ increase in the $t_{1/2}$ (time to decay by 50%) of PP EPSPs relative to control (TRIP8b siRNA: 28.36 ± 1.26 ms, $n = 15$; control siRNA: 47.79 ± 2.92 ms, $n = 18$; $p < 0.01$; Figure 1H). Addition of ZD7288 increased the $t_{1/2}$ further, and to identical values in both populations of neurons (TRIP8b siRNA: 62.91 ± 1.47 ms; $n = 15$; control: 63.45 ± 2.14 ms; $n = 18$). These results are consistent with the view that a reduction of TRIP8b protein in CA1 pyramidal neurons in vivo causes a substantial and specific decrease in somatodendritic Ih.

Reduction of TRIP8b Disrupts HCN1 Protein Trafficking in CA1 Pyramidal Neurons

To examine how reduction in TRIP8b causes loss of Ih, we used immunohistochemistry to examine the expression and localization of HCN1 protein (the predominant HCN isoform in pyramidal neurons) following siRNA-mediated knockdown of TRIP8b. Viral expression of TRIP8b siRNA, but not control siRNA, caused a marked redistribution of HCN1 in CA1 neurons, with

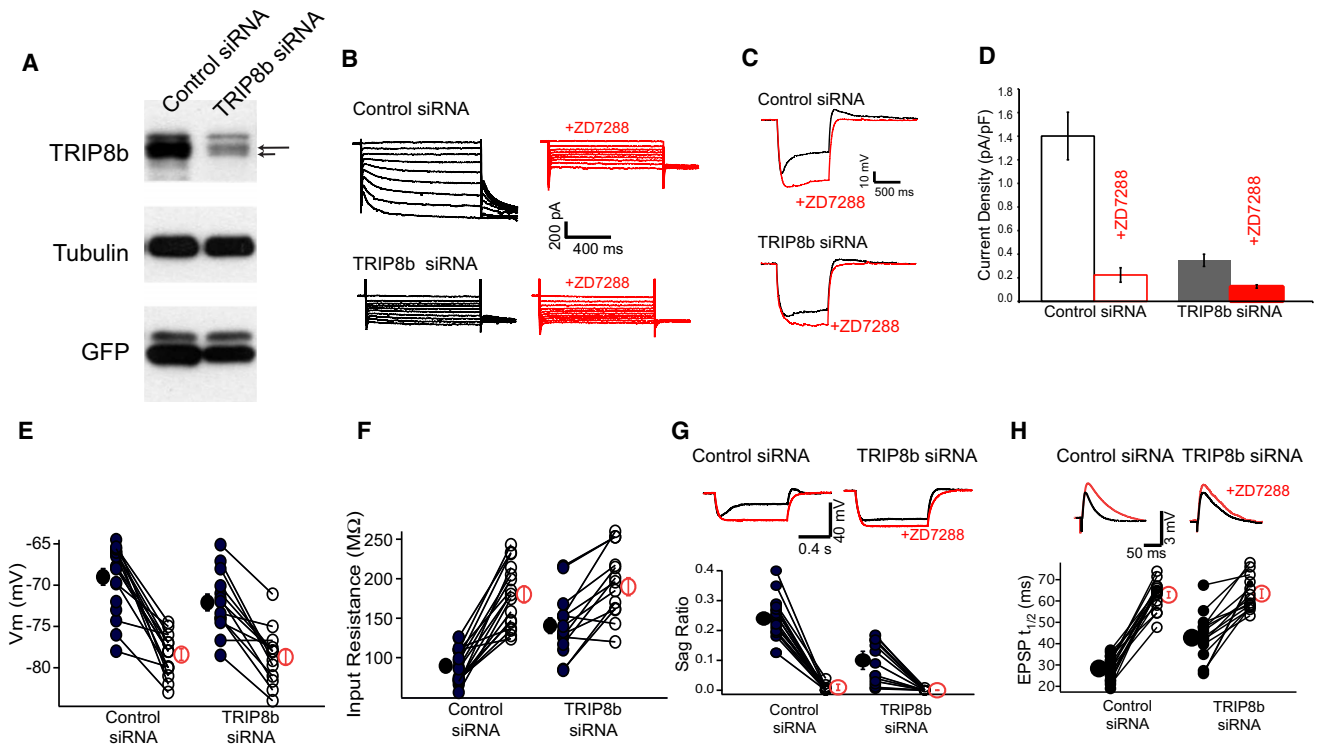


Figure 1. Expression of TRIP8b siRNA Alters the Electrophysiological Properties of CA1 Neurons Consistent with a Reduction in Ih In Vitro and In Vivo

(A) Western blot of total protein extracts from hippocampal neuron cultures 18 days in vitro infected with lentiviral vectors expressing EGFP plus either control siRNA or TRIP8b siRNA. Note that TRIP8b siRNA reduced TRIP8b levels with no change in tubulin from cultures expressing roughly equal amounts of EGFP. The long arrow points to the TRIP8b(1a-4) band and the short arrow to TRIP8b(1a).

(B) Voltage clamp recordings from dissociated hippocampal cultures show reduction in Ih with TRIP8b siRNA compared with control siRNA, before and after application of 10 μ M ZD7288. Currents elicited by 3 s hyperpolarizing voltage steps from holding potential of -40 mV to -130 mV in 10 mV increments.

(C) Current clamp recordings from dissociated hippocampal cultures show voltage responses to a -80 pA hyperpolarizing current step before and after application of 10 μ M ZD7288.

(D) Mean Ih current density from cells expressing control or TRIP8b siRNAs, before and after application of 10 μ M ZD7288 (mean \pm SEM).

(E–H) Electrophysiological properties of CA1 pyramidal neurons in acute slices expressing either control or TRIP8b siRNAs. Lines connect individual data points (small circles) from same slice in absence or presence of 10 μ M ZD7288. Large circles: mean \pm SEM.

(E) Resting membrane potential.

(F) Input resistance (measured with a 500 ms -50 pA hyperpolarizing current step).

(G) Sag ratio (see Experimental Procedures). Traces show voltage responses to hyperpolarizing current pulses from a holding potential of -70 mV in absence (black traces) or presence (red traces) of 10 μ M ZD7288 from cells expressing control (left) or TRIP8b (right) siRNA.

(H) Somatic EPSP decay time ($t_{1/2}$). Traces show somatic EPSPs in response to PP stimulus from cells expressing control (left) or TRIP8b (right) siRNAs, either in absence (black traces) or presence (red traces) of 10 μ M ZD7288.

a significant increase in channel staining in the somatic layer and proximal dendrites in SR, compared with uninfected neurons in the same slice (Figure 2A). High magnification z-series sections revealed the appearance of HCN1 in discrete puncta in the cytoplasm surrounding the nucleus of neurons expressing the TRIP8b siRNA (Figure 2B). Such puncta were not observed in neighboring uninfected cells or in neurons infected with control siRNA.

These results were quantified by measuring the intensity of HCN1 staining in the pyramidal layer (SP), proximal dendrites (SR) and distal dendrites (SLM) of infected (EGFP +) and uninfected (EGFP -) CA1 neurons (Figure 2C). There was no significant difference in HCN1 staining between uninfected cells and cells infected with control siRNA. However, cells infected with

TRIP8b siRNA exhibited a 43% increase in HCN1 staining intensity in the soma and a 22% increase in the SR, compared with uninfected neighboring cells in the same slice (N = 6 mice, 12 injections sites for TRIP8b siRNA, N = 4 mice, 8 injections sites for control). Each data point is the average of 17 regions. In contrast, there was no detectable difference in staining intensity in SLM between regions infected with TRIP8b siRNA versus uninfected regions.

The punctate pattern of HCN1 suggests that the increase in staining in the soma and proximal dendrites results from channel accumulation in an intracellular compartment, consistent with the observed decrease in Ih (see Figures 1D–1H). These results imply that a reduction in TRIP8b expression produces a defect in HCN1 membrane trafficking. The lack of change in HCN1 in

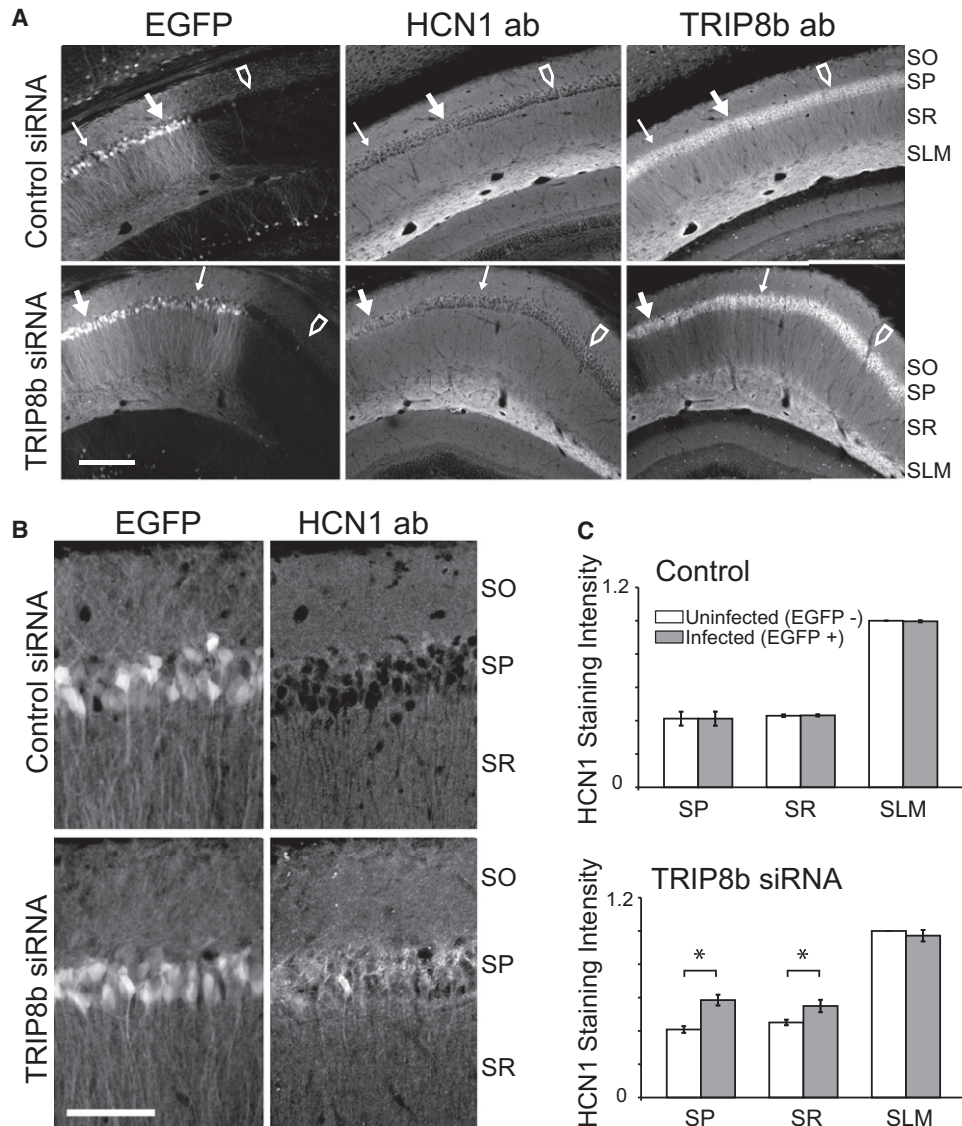


Figure 2. In Vivo siRNA-Mediated Knockdown of TRIP8b Reduces Its Protein Levels and Leads to Redistribution of HCN1

(A) Expression pattern of EGFP, HCN1 or TRIP8b in CA1 region of hippocampal slices from brains of mice in which lentiviral vectors expressing control siRNA (top row) or TRIP8b knockdown siRNA (bottom row) were injected stereotactically in CA1. *Left column*, Images of EGFP fluorescence reveal variable pattern of viral expression, which ranged across transverse axis of a hippocampal slice from regions with very high siRNA expression (thick solid arrow), to regions with intermediate expression (thin arrow), to regions with undetectable viral infection (open arrow). *Right column*, Levels of TRIP8b detected by immunohistochemistry were decreased in region of slice where viral expression (EGFP signal) was highest (thick solid arrow). Levels of TRIP8b were unaffected in region of slice where viral expression was undetectable (open arrow). *Middle column*, Levels of HCN1 increased in somatic layer of CA1 where viral expression was very high (thick solid arrow). The scale bar represents 300 μ m.

(B) Higher-magnification z-series projections showing specific redistribution of HCN1 protein into the somatic layer of CA1 pyramidal cells infected with TRIP8b knockdown siRNA. Note lack of somatic staining with control siRNA. The scale bar represents 10 μ m.

(C) Quantification of HCN1 staining in the SP, SR and SLM regions of CA1 infected with control (top) or anti-TRIP8b (bottom) siRNAs. EGFP-positive regions were compared with EGFP- negative regions in same slice. HCN1 fluorescence intensity was normalized by setting the maximal intensity of the image to 1. Note significant increase in relative staining in soma and SR of slices expressing TRIP8b siRNA (* $p < 0.05$; t test).

SLM may reflect technical limitations of the immunohistochemical approach to detect a redistribution of HCN1 from the membrane to cytoplasmic compartments in the thin distal dendrites. In addition, high levels of background HCN1 staining in lateral dendritic branches from uninfected neurons may

prevent the detection of changes in channel expression in those neurons infected with virus. Finally, the interaction of TRIP8b with HCN1 in distal dendrites may be extremely stable and persist even when the pool of available TRIP8b is decreased (Santoro et al., 2009).

Knockdown of TRIP8b Impairs the Expression of EGFP-HCN1 in CA1 Distal Dendrites

To overcome some of the above limitations of immunohistochemistry, we coinjected slices with viral vectors expressing siRNA and EGFP-tagged HCN1 (EGFP-HCN1). To prevent interference from endogenous HCN1, we performed these experiments in HCN1 knockout mice (Nolan et al., 2003; Santoro et al., 2009). With the siRNA vector, a separate vector expressed the soluble red fluorescent protein, DsRed2. We were therefore able to examine channel distribution (green fluorescence) only from those neurons coinjected with siRNA (red fluorescence). Because we coinjected independent lentiviral vectors to coexpress EGFP-HCN1 with siRNA, we could selectively monitor the effect of TRIP8b knockdown on channels that were synthesized de novo when endogenous levels of TRIP8b were being reduced.

We previously found (Santoro et al., 2009) that virally expressed EGFP-HCN1 (in the background of the HCN1 KO mouse) is properly trafficked to the distal apical dendrites of CA1 pyramidal neurons in a gradient of increasing expression that closely resembles the profile of endogenous HCN1 (Lorincz et al., 2002; Notomi and Shigemoto, 2004; Santoro et al., 1997). In contrast, DsRed2 is expressed uniformly throughout the somatodendritic compartments (Figure 3A, center panels). Although the dendritic targeting of EGFP-HCN1 was unaltered by control siRNA, it was markedly perturbed by TRIP8b siRNA, which greatly reduced EGFP fluorescence in distal CA1 dendrites with no detectable change in soma and proximal dendrites (Figure 3A, left panels).

We analyzed the profile of channel expression by plotting the ratio of EGFP-HCN1 to DsRed2 fluorescence as a function of distance along the somatodendritic longitudinal axis (Figure 3B). In slices that had been infected with control siRNA, this ratio was relatively constant in the soma and proximal dendrites of SR and increased steeply in the distal regions of SR into SLM, reflecting the normal gradient of endogenous HCN1. TRIP8b knockdown had little effect on the EGFP-HCN1 to DsRed2 fluorescence ratio in the soma and proximal dendrites of SR. However, there was a large decrease in the EGFP-HCN1 to DsRed2 ratio in the distal regions of SR and throughout SLM. A comparison of the ratio in slices expressing control siRNA to the ratio in slices expressing TRIP8b siRNA confirmed that downregulation of TRIP8b produced a selective reduction in channel expression in CA1 distal dendrites (Figure 3C, N = 5 mice, 10 injection sites for TRIP8b siRNA and 4 mice, 8 injection sites for control). This altered ratio was not caused by changes in dendritic architecture as the DsRed2 distribution was unaffected by the siRNA.

In summary, siRNA-mediated reduction of TRIP8b resulted in a marked loss of HCN1 in the plasma membrane as detected by several electrophysiological parameters that reflect Ih. Furthermore, knockdown of TRIP8b in vivo resulted in an increased immunoreactivity for HCN1 channels in the CA1 soma and proximal dendrites that represents a redistribution of HCN1 to intracellular compartments. Additionally, coexpression of EGFP-HCN1 with TRIP8b siRNA revealed a selective loss of channel fluorescence in SLM. All together, these results indicate that, in addition to being important for HCN1 expression on the

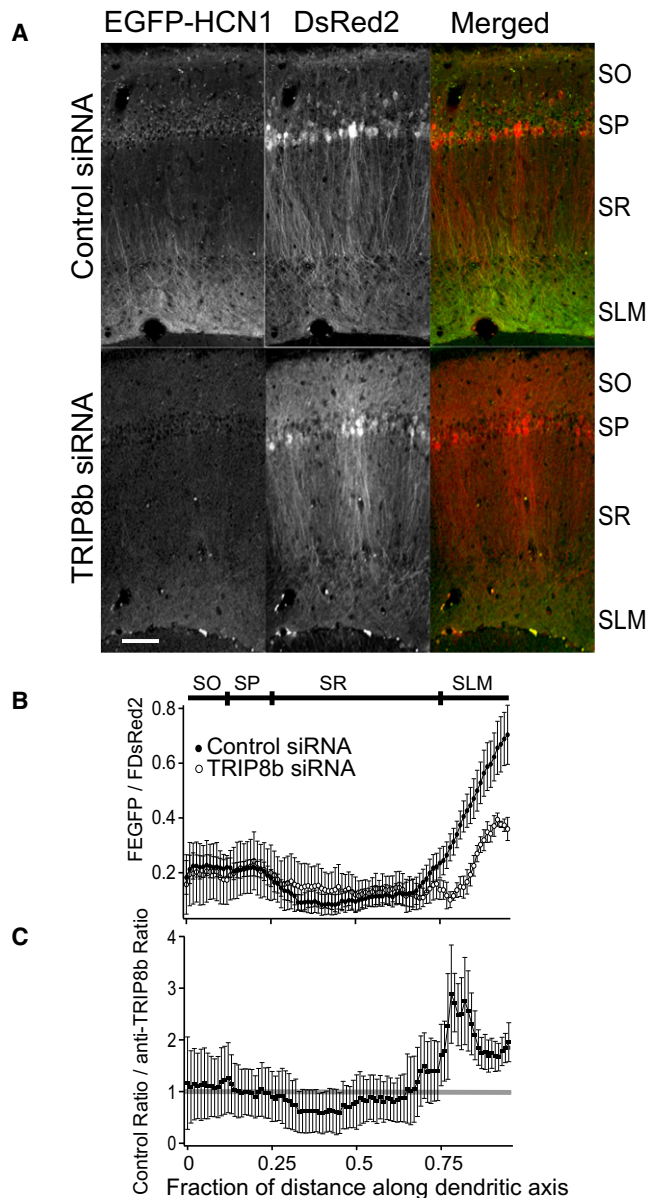


Figure 3. TRIP8b siRNA Impairs the Dendritic Expression of EGFP-HCN1 in HCN1 KO Mice

(A) EGFP-HCN1 was coexpressed with either control (top row) or TRIP8b (bottom row) siRNAs using independent lentiviral vectors in HCN1 KO mice. Left column: Fluorescence signal from EGFP-HCN1. Middle column: DsRed2 signal (expressed from siRNA vector). Right column: merged signal showing EGFP-HCN1 (green) and DsRed2 (red). Note effect of TRIP8b siRNA to reduce EGFP-HCN1 signal, especially in distal dendrites. The scale bar represents 100 μ m.

(B) Ratio of EGFP-HCN1 to DsRed2 fluorescence as function of distance along somatodendritic axis in slices infected with control (filled symbols) or TRIP8b (open symbols) siRNAs. Symbols show mean; error bars show SEM.

(C) EGFP-HCN1/DsRed2 ratio from slices infected with control siRNA divided by ratio from slices infected with TRIP8b siRNA. Note selective decrease in HCN1 staining in distal dendrites of SR and SLM. (Error bars, SEM). The horizontal gray line indicates a ratio of 1.

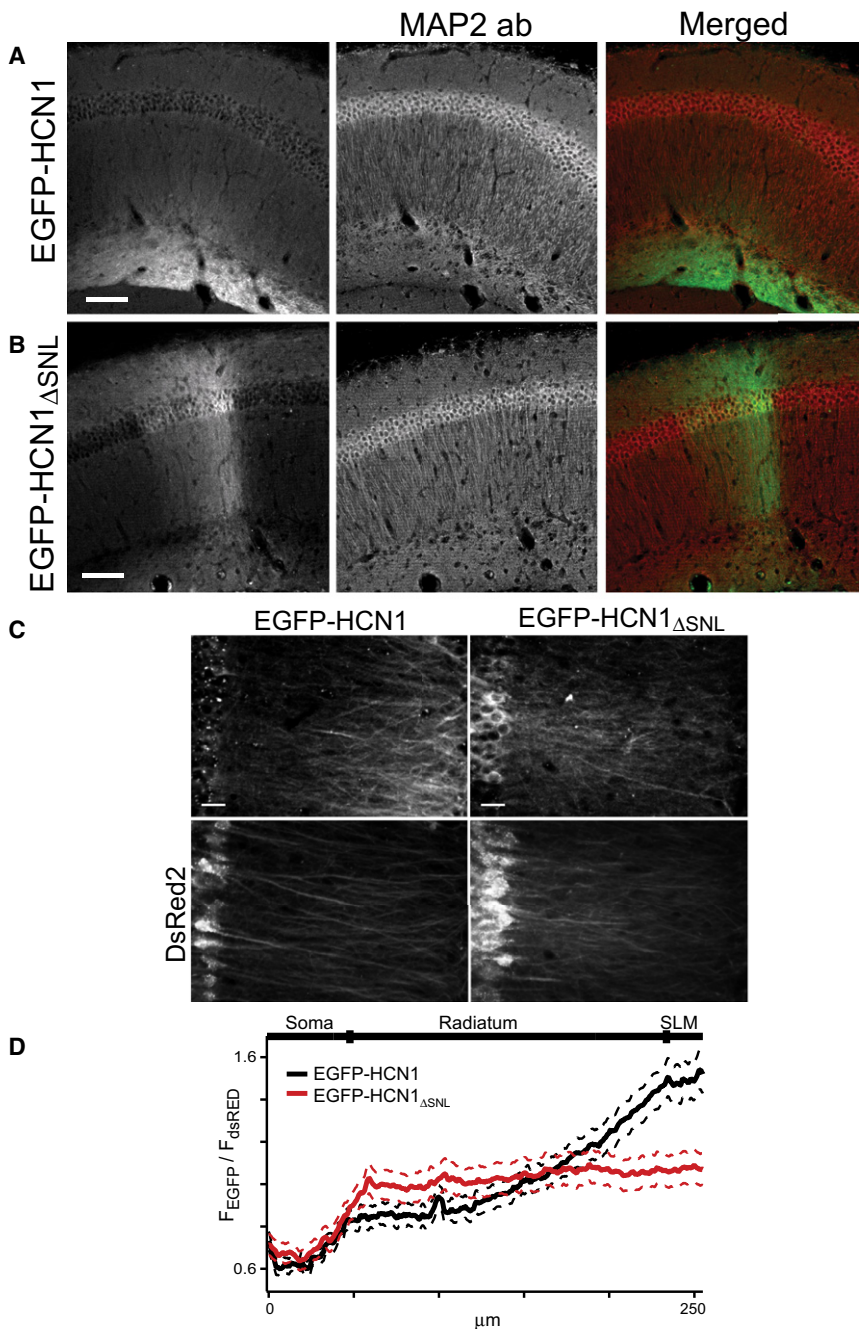


Figure 4. HCN1 Δ SNL Truncation Mutant Shows Defective Trafficking to CA1 Distal Dendrites

(A and B) Images of CA1 region from hippocampal slices from HCN1 KO mouse expressing EGFP-HCN1 (A) or EGFP-HCN1 Δ SNL (B). EGFP-tagged channel fluorescence (left column) and as green (right column). Staining for MAP2 dendritic marker (middle column) and as red (right). Note that full-length EGFP-HCN1 was trafficked efficiently to distal apical dendrites whereas EGFP-HCN1 Δ SNL showed even dendritic distribution, with relatively high expression in soma and proximal apical and basal dendrites. The scale bar represents 200 μm . (C) Higher magnification z-series projections showing fluorescence signals for EGFP-HCN1, EGFP-HCN1 Δ SNL, and coexpressed DsRed2. The scale bar represents 10 μm .

(D) EGFP and DsRed2 fluorescence intensities were measured along somato-dendritic axis in soma and apical dendrites of individual cells. Mean EGFP signal averaged from individual dendrites was normalized by DsRed2 signal and plotted as function of distance from somatic layer for neurons expressing EGFP-HCN1 (black) or EGFP-HCN1 Δ SNL (red). (Solid lines: means; dashed lines: SEM).

protein that interacts with HCN1. To address these questions, we adopted a third, complementary approach, discussed next.

A C-Terminal EGFP-HCN1 Truncation Mutant with Impaired Binding to TRIP8b Shows Impaired Targeting to CA1 Distal Dendrites

To overcome the limitations of the siRNA approach, we expressed an EGFP-tagged HCN1 truncation mutant (EGFP-HCN1 Δ SNL) that lacks the HCN1 C-terminal SNL tripeptide required for high affinity binding of HCN1 to TRIP8b (Santoro et al., 2004, 2011; Lewis et al., 2009). We observed a dramatic loss of dendritic targeting when we expressed EGFP-HCN1 Δ SNL in the background of HCN1 KO mice (Figures 4A and 4B). Unlike wild-type HCN1, the mutant channel was expressed uniformly at high

plasma membrane, TRIP8b may also be important for the targeting of HCN1 to distal dendrites. However, the loss of HCN1 in distal dendrites might not reflect a specific role of TRIP8b in dendritic targeting but may be secondary to the general loss of HCN1 surface expression upon TRIP8b knockdown. Moreover, because the TRIP8b siRNA reduced but did not eliminate TRIP8b protein, it is unclear whether the residual targeting of HCN1 to the distal dendrites results from an effect of residual TRIP8b or represents the action of some other targeting

levels throughout CA1, as evident in the relatively constant EGFP-HCN1 Δ SNL to DsRed2 fluorescence ratio along the somato-dendritic axis. A comparison with the distribution of full-length HCN1 revealed not only a loss of expression of the mutant channel in the distal dendrites but also an increase in expression in proximal dendrites (Figures 4C and 4D; EGF-HCN1: N = 4 mice, 8 injection sites; EGFP-HCN1 Δ SNL: N = 5 mice, 10 injection sites). As TRIP8b is the major protein that interacts with the HCN C terminus in the brain (Santoro et al., 2004, 2009; Zolles

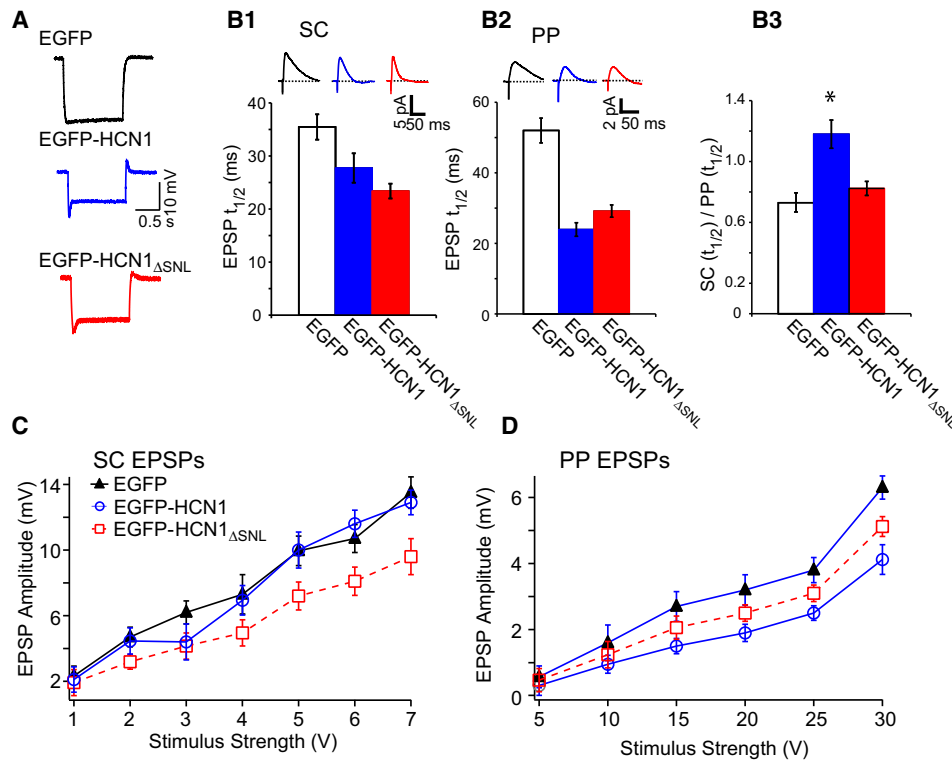


Figure 5. Whole-Cell Recordings from CA1 Neurons Expressing EGFP-HCN1 or EGFP-HCN1 $_{\Delta SNL}$ Indicate that the SNL Deletion Results in a Mistargeting of HCN1

A series of electrophysiological properties were determined for CA1 pyramidal neurons from HCN1 KO mice expressing EGFP (control, black), EGFP-HCN1 (blue) or EGFP-HCN1 $_{\Delta SNL}$ (red). (A) Somatic voltage traces from whole-cell current-clamp recordings showing expression of full-length or truncated HCN1 resulted in a prominent depolarizing voltage sag in response to 100 pA hyperpolarizing current steps from a holding potential of -70 mV. (B) Expression of EGFP-HCN1 and EGFP-HCN1 $_{\Delta SNL}$ differentially enhanced $t_{1/2}$ decay time of EPSPs in response to stimulation of proximal (SC) inputs (B1) versus distal (PP) inputs (B2). (B3) Ratio of SC/PP EPSP $t_{1/2}$ values was significantly different following expression of EGFP-HCN1 versus EGFP-HCN1 $_{\Delta SNL}$. Peak amplitude input-output curves for SC (C) and PP (D) EPSPs from CA1 pyramidal neurons expressing EGFP (black triangles), EGFP-HCN1 (blue circles) or EGFP-HCN1 $_{\Delta SNL}$ (red squares). (Error bars: SEM).

et al., 2009), these results strongly implicate TRIP8b as a key element necessary for the efficient targeting of HCN1 channels to distal portions of CA1 pyramidal neuron apical dendrites.

CA1 Neurons Expressing EGFP-HCN1 $_{\Delta SNL}$ Display Altered Physiological Properties Consistent with Channel Mistargeting

Because of the limitations of fluorescence imaging, we used an electrophysiological approach to measure EGFP-HCN1 $_{\Delta SNL}$ channel levels in the surface membrane in HCN1 KO mice. The resting potential of neurons expressing EGFP-HCN1 $_{\Delta SNL}$ (-69.2 ± 1.2 ; $n = 13$) was identical to that of neurons expressing EGFP-HCN1 (-69.1 ± 1.1 mV; $n = 15$), and both were ~ 14 mV more positive than the resting potential of control neurons from the HCN1 knockout mice expressing EGFP (-82.7 ± 1.5 mV; $n = 15$; $p < 0.01$ relative to full-length and mutant channels). This suggests that the wild-type and mutant channels produced similar increases in somatic Ih. Expression of full-length and mutant channels also led to similar, significant decreases in input resistance (EGFP-HCN1 $_{\Delta SNL}$: 107.2 ± 15.7 M Ω , $n = 13$; EGFP-HCN1: 109.1 ± 7 M Ω , $n = 15$) relative to that of control neurons

expressing EGFP (149.6 ± 14 M Ω , $n = 15$; $p < 0.01$). Finally, sag ratios were similarly enhanced (Figure 5A) in neurons expressing EGFP-HCN1 (0.23 ± 0.03 , $n = 15$) or EGFP-HCN1 $_{\Delta SNL}$ (0.22 ± 0.02 , $n = 13$), relative to that in control neurons from the knockout mice (0.05 ± 0.01 , $n = 15$; $p < 0.01$). Thus, expression of EGFP-HCN1 and EGFP-HCN1 $_{\Delta SNL}$ in HCN1 KO mice yielded large, nearly identical levels of Ih when measured at the soma.

Next, we assessed levels of Ih in CA1 proximal and distal dendrites, based on the time course of decay of SC and PP EPSPs (Figure 5B). In control knockout neurons expressing EGFP, the $t_{1/2}$ of the SC EPSP (35 ± 2 ms) was significantly faster than that of the PP EPSP (52 ± 4 ms; $n = 15$; $p < 0.05$), as expected from the passive cable properties of the dendrite. Expression of either EGFP-HCN1 or EGFP-HCN1 $_{\Delta SNL}$ led to a speeding of the decay of the SC EPSP, although EGFP-HCN1 $_{\Delta SNL}$ produced a significantly larger speeding of the $t_{1/2}$ (23 ± 1 ms; $n = 13$) relative to the $t_{1/2}$ with EGFP-HCN1 (27.7 ± 3 ms; $n = 15$; $p < 0.05$, compared with EGFP and EGFP-HCN1; ANOVA, Tukey HSD). In contrast we observed the opposite pattern for PP EPSPs; EGFP-HCN1 produced a significantly larger speeding ($t_{1/2}$ of 24 ± 2 ms; $n = 15$) compared with the

truncated channel ($t_{1/2}$ of 29 ± 2 ms; $n = 13$; $p < 0.05$, ANOVA Tukey HSD). The differential effect of full-length versus mutant HCN1 on the decay of the PP versus SC EPSP was apparent when we compared the ratio of SC EPSP to PP EPSP decay times in neurons expressing EGFP, EGFP-HCN1 and EGFP-HCN1 $_{\Delta\text{SNL}}$ (Figure 5B3). Whereas full-length HCN1 preferentially sped the decay of the PP EPSP relative to the SC EPSP, the mutant channel produced a similar speeding of EPSPs in both pathways.

As a final assay of functional levels of Ih in dendritic compartments, we compared the effects of the three different constructs on the input-output curves for SC and PP EPSP peak amplitude, as this parameter is reduced by high levels of HCN1 (George et al., 2009; Magee, 1998). EGFP-HCN1 had no effect on the input-output curve for SC EPSPs (Figures 5C and 5D), consistent with the relatively low levels of full-length HCN1 in proximal dendrites. In contrast, EGFP-HCN1 $_{\Delta\text{SNL}}$ decreased significantly the SC EPSP amplitude, relative to the EPSP in either control knockout neurons expressing EGFP or neurons expressing full-length EGFP-HCN1 ($p < 0.01$, ANOVA with Tukey's HSD test, stimulus strengths >4 V) (Figure 5D). In contrast, EGFP-HCN1 caused a large reduction of the PP EPSP ($p < 0.01$, ANOVA with Tukey's HSD test relative to EGFP control EPSPs, stimulus strengths >15 V) that was significantly greater than the reduction seen with EGFP-HCN1 $_{\Delta\text{SNL}}$ ($p < 0.05$ ANOVA with Tukey's HSD, 25 and 30 V stimulus strengths).

These results demonstrate that while full-length HCN1 is targeted to CA1 distal dendrites, the truncation mutant is expressed at high, relatively uniform levels in the somatodendritic membrane throughout the CA1 neuron, consistent with our results based on EGFP fluorescence. Thus, the loss of distal dendritic targeting of HCN1 $_{\Delta\text{SNL}}$ is not secondary to loss of membrane surface expression but must represent the loss of a primary action of TRIP8b to target full-length HCN1 to distal dendrites. As downregulation of TRIP8b with siRNA decreases HCN1 surface expression, the HCN1 $_{\Delta\text{SNL}}$ results further indicate that the actions of TRIP8b to enable proper surface membrane expression and to direct distal dendritic targeting of HCN1 are dissociable functions. This is consistent with recent reports that HCN1 and TRIP8b interact at two distinct sites (Lewis et al., 2009; Santoro et al., 2011) and that the weakened binding between TRIP8b and HCN1 $_{\Delta\text{SNL}}$ is sufficient to allow certain TRIP8b isoforms to enhance surface expression of the mutant channel (see Discussion).

Which TRIP8b Splice Isoforms Are Important for HCN1 Trafficking?

Although our results indicate that TRIP8b is critical for the proper surface expression and dendritic targeting of HCN1 in CA1 pyramidal neurons, these data do not provide insight as to which specific TRIP8b isoform (or combination of isoforms) is involved. The identification of the role of individual isoforms is a daunting task as there are at least ten different splice variants of TRIP8b expressed in brain (Lewis et al., 2009; Santoro et al., 2009). Moreover, the small size of the various alternatively spliced exons makes it impractical to design selective siRNAs to knock-down specific isoforms. Nonetheless, we obtained insight into the function of specific isoforms by examining a mouse line,

Pex51^{tm1(KOMP)Vlcg}, in which exons 1b and 2 in the TRIP8b gene were replaced by lacZ through homologous recombination (<http://www.komp.org>; Figure S2). The removal of all splice forms containing exons 1b or 2 is expected to delete all except three of the TRIP8b splice isoforms, namely TRIP8b(1a), TRIP8b(1a-4) and TRIP8b(1a-3-4). Of these, TRIP8b(1a) and TRIP8b(1a-4) are the most abundant splice forms in the mouse brain, accounting for 25%–30% and 30%–40%, respectively, of total TRIP8b mRNA. In contrast, TRIP8b(1a-3-4) is normally expressed at very low levels in brain ($<5\%$ of total brain TRIP8b mRNA; (Santoro et al., 2009) and is not detected in hippocampus (Lewis et al., 2009).

The TRIP8b exon 1b/2 KO mice are generally viable, with normal body weight and overall brain structure. Western blot analysis of brain extracts from these mice confirmed the loss of all TRIP8b isoforms containing exons 1b or 2. In contrast, the hippocampal TRIP8b isoforms lacking these exons, TRIP8b(1a) and TRIP8b(1a-4), showed strong signals on western blots of brain extracts from the knockout mice, although the levels of expression of these isoforms were reduced somewhat compared with those seen in wild-type littermates (Figure S2). Moreover, the remaining TRIP8b splice forms showed a normal dendritic pattern of immunohistochemical staining in the CA1 region of the KO mice (Figure 6A; see also Figures S3 and S4).

Remarkably, despite the loss of all but two of the hippocampal TRIP8b isoforms, the endogenous expression pattern of HCN1 in the CA1 region of the KO mice was identical to that of wild-type mice, with the characteristic dendritic gradient of HCN1 expression (Figures 6C and 6D; see also Figure S4). Combined with our above results using siRNA and EGFP-HCN1 $_{\Delta\text{SNL}}$, which demonstrated the general importance of TRIP8b isoforms for HCN1 expression and dendritic targeting, the results from the 1b/2 KO mice indicate that TRIP8b(1a-4) and/or TRIP8b(1a) must be the key isoforms that regulate HCN1 trafficking in CA1 neurons.

What is the role of the TRIP8b isoforms containing exons 1b or 2? Although the endogenous staining pattern with the pan-TRIP8b antibody in CA1 was very similar in the knockout and control animals, labeling disappeared in the KO mice from a distinct population of small cells enriched in the dentate gyrus and CA3 regions (Figure 6B). These cells, present throughout the brain, are likely oligodendrocytes, as they were colabeled with an antibody to 2', 3'-cyclic nucleotide 3'-phosphodiesterase (CNPase), an oligodendrocyte-specific marker (Figure S3). Furthermore, we detected β -galactosidase (which replaced exons 1b/2 in the KO mice, see Figure S2) in these cells of the 1b/2 KO animals, indicating that these cells normally express exons 1b and 2 (Figure S3). Although oligodendrocytes do not express HCN1, they do express HCN2 (Notomi and Shigemoto, 2004), which also interacts strongly with TRIP8b (Santoro et al., 2004; Zolles et al., 2009).

TRIP8b(1a-4) and TRIP8b(1a) Are Expressed in CA1 Neuron Axonal-Dendritic Compartments

To elucidate further the potential role of TRIP8b(1a) and TRIP8b(1a-4) in the trafficking of HCN1 in the hippocampus, we examined their endogenous localization in wild-type and KO mice using exon-specific antibodies. We first studied

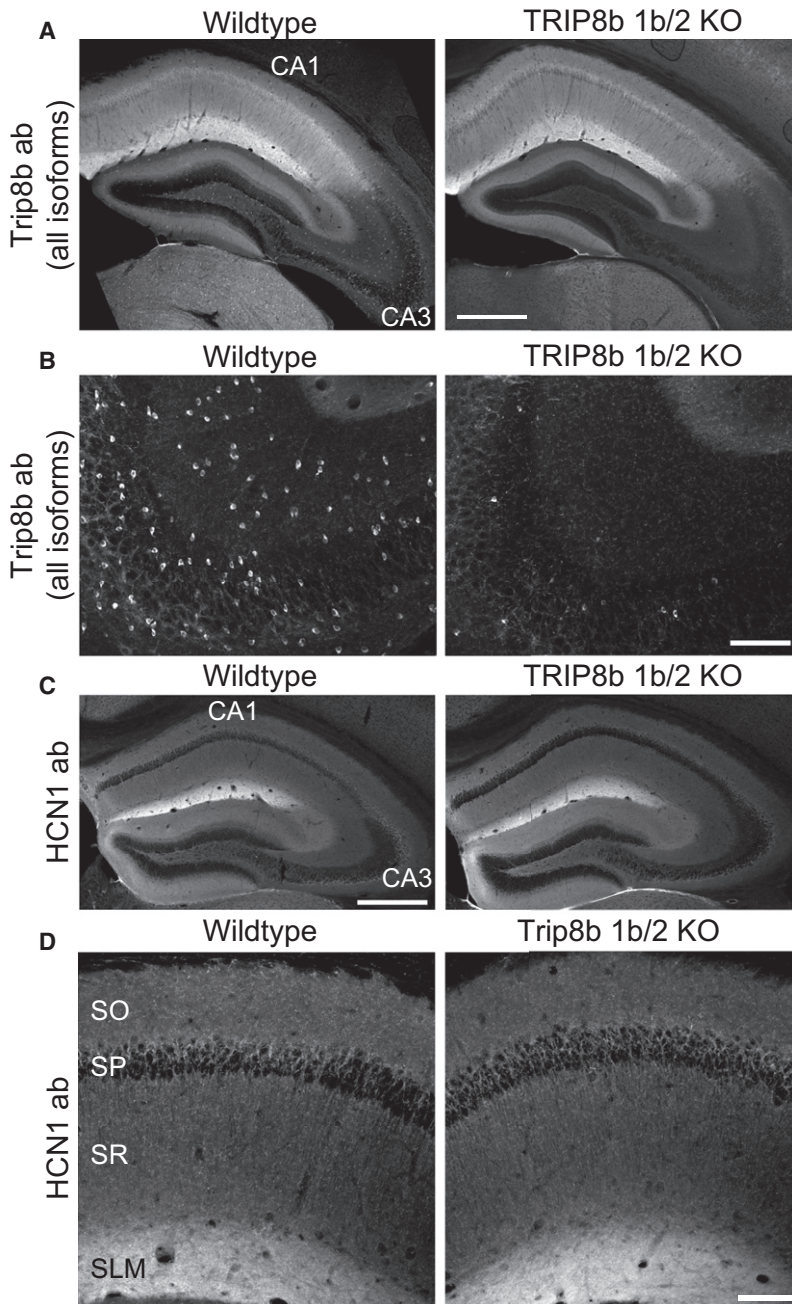


Figure 6. Expression of TRIP8b and HCN1 in Hippocampal Slices from TRIP8b Exon 1b/2 Knockout Mice

(A) Coronal hippocampal sections from wild-type and TRIP8b exon 1b/2 knockout mice littermates. Slices were labeled with a monoclonal pan-TRIP8b antibody that binds to all isoforms. The scale bar represents 500 μ m.

(B) Higher magnification z-axis projection of area CA3 from wild-type and TRIP8b 1b/2 KO mice, showing loss of pan-TRIP8b staining from small glial-like cells following deletion of exons 1b and 2. The scale bar represents 100 μ m.

(C) Immunolabelling of slices from wild-type and TRIP8b 1b/2 KO littermates mice showing a normal expression pattern of endogenous HCN1 throughout the hippocampus. The scale bar represents 500 μ m.

(D) Higher magnification z-axis projection of area CA1 showing the identical targeting of HCN1 to distal dendrites in SLM of wild-type and TRIP8b 1b/2 KO mice. The scale bar represents 100 μ m.

staining pattern for exon 4 was identical in wild-type and 1b/2 knockout mice (Figure S4). Thus, the exon 4 antibody signal in wild-type animals is likely to predominantly represent staining for TRIP8b(1a-4), as all other exon 4-containing isoforms normally expressed in hippocampus were deleted in the knockout mice. These immuno-histochemistry data, together with previous findings that TRIP8b(1a-4) promotes HCN1 surface expression in heterologous cells (Lewis et al., 2009; Santoro et al., 2009), suggest that TRIP8b(1a-4) is likely to be a key TRIP8b isoform that promotes the surface expression and efficient targeting of HCN1 to the CA1 distal dendrites.

Next we examined the expression pattern of TRIP8b(1a) using a chicken polyclonal antibody recognizing a peptide corresponding to the junction of exons 1a and 5. This antibody preferentially detected TRIP8b(1a) over TRIP8b(1a-4), based on western blot analysis, and detected virally expressed TRIP8b(1a) in CA1 neurons by immunohistochemistry (Figure S5). The staining pattern with the TRIP8b(1a) antibody was distinct and remarkably complementary to both the staining with the exon 4 antibody and the staining pattern of HCN1. Thus, in the hippocampus, TRIP8b(1a) was detected at highest levels in the alveus, where TRIP8b(1a-4) and HCN1 staining were lacking. Although the TRIP8b(1a) antibody did stain the SLM of CA1 and subiculum (Figure 7C), high magnification z-axis projections revealed that the TRIP8b(1a) signal was present in dense bundles of fibers running semiperpendicularly to the dendritic axis of the CA1 pyramidal neurons (Figure 7D). This is distinct from the diffuse SLM signal seen with the antibody against exon 4. Sparse fibers were also detected with the TRIP8b(1a) antibody in SR and SO. TRIP8b(1a)-labeled fibers were colabeled with an antibody to intermediate-sized neurofilament, an axonal marker (Figure S6).

immunohistochemical staining with a mouse monoclonal antibody that specifically recognizes exon 4. In hippocampal slices from wild-type mice, exon 4 labeling was detected in a pattern very similar to that of endogenous HCN1. Thus, labeling was present at highest levels in the SLM of CA1 and subiculum, with a sharp cutoff in signal at the CA1-CA2 border (Figures 7A and 7B). Although four TRIP8b splice isoforms that contain exon 4 (TRIP8b(1a-2-3-4), TRIP8b(1a-2-4), TRIP8b(1a-4), and TRIP8b(1b-2-4)) are normally expressed in hippocampus (Santoro et al., 2009), TRIP8b(1a-4) is by far the most abundant (Santoro et al., 2009). Moreover, we found that the hippocampal

immunohistochemical staining with a mouse monoclonal antibody that specifically recognizes exon 4. In hippocampal slices from wild-type mice, exon 4 labeling was detected in a pattern very similar to that of endogenous HCN1. Thus, labeling was present at highest levels in the SLM of CA1 and subiculum, with a sharp cutoff in signal at the CA1-CA2 border (Figures 7A and 7B). Although four TRIP8b splice isoforms that contain exon 4 (TRIP8b(1a-2-3-4), TRIP8b(1a-2-4), TRIP8b(1a-4), and TRIP8b(1b-2-4)) are normally expressed in hippocampus (Santoro et al., 2009), TRIP8b(1a-4) is by far the most abundant (Santoro et al., 2009). Moreover, we found that the hippocampal

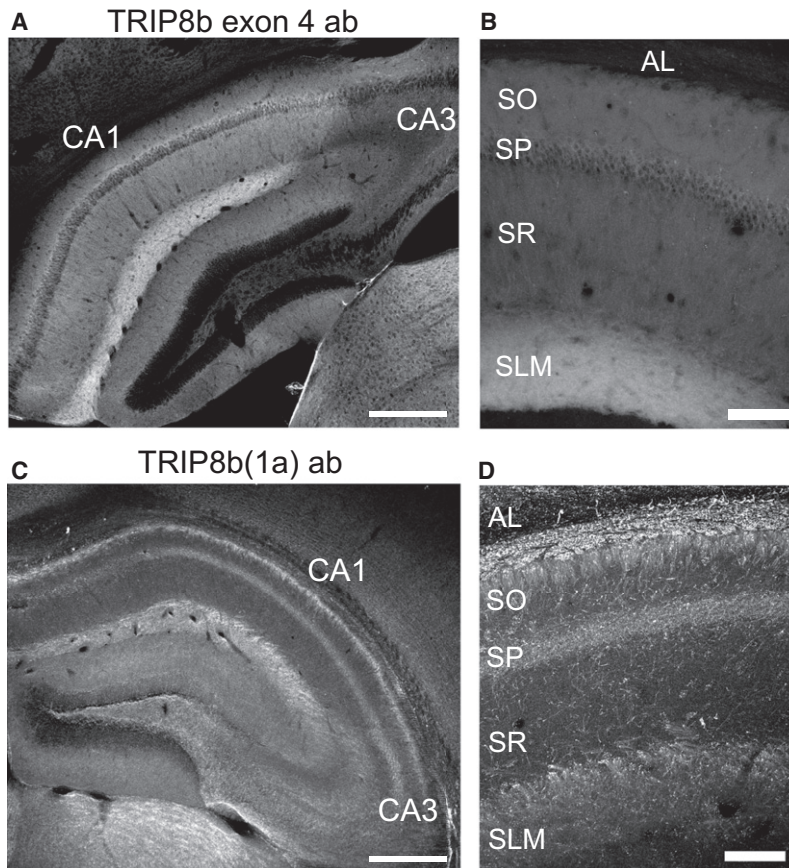


Figure 7. The Endogenous Expression Patterns of TRIP8b Isoforms Containing Exon 4 and TRIP8b(1a) Show Complementary Localization

(A) Coronal brain sections immunolabeled with an antibody specific to exon 4 of TRIP8b. Strongest signal was seen in distal dendrites of CA1 in SLM. The scale bar represents 500 μ m.

(B) Higher-magnification z-projection image of CA1 neurons immunolabeled with antibody to TRIP8b exon 4. The scale bar represents 100 μ m.

(C) Immunolabeling with an antibody recognizing TRIP8b(1a). Note the high expression in the alveus of the hippocampus. The scale bar represents 500 μ m.

(D) Higher magnification images reveal that TRIP8b(1a) is localized to fiber bundles in SO, SLM and in sparse fibers in SR. The scale bar represents 100 μ m.

These results suggest that TRIP8b(1a) is present in axonal fibers, including those of CA1 pyramidal cells, which project through the alveus. Of interest, little or no staining for endogenous HCN1 was detected in such fibers, as seen by comparing Figure 6D with Figure 7D. Given that TRIP8b(1a) downregulates HCN1 surface expression in *Xenopus* oocytes (Santoro et al., 2009), our findings suggest that TRIP8b(1a) may act to suppress HCN1 channel misexpression in CA1 neuron axons.

Effects of Overexpression of HA-Tagged TRIP8b(1a-4) and TRIP8b(1a) on EGFP-HCN1 Trafficking in Dendrites of CA1 Pyramidal Neurons

To test the hypothesis that TRIP8b(1a-4) enhances HCN1 surface expression and targets the channel to its proper dendritic locale whereas TRIP8b(1a) prevents axonal expression of the channel, we examined the effects of viral overexpression of these two TRIP8b isoforms, both fused to an HA tag to allow us to distinguish exogenous from endogenous protein. In a previous study (Santoro et al., 2009), coexpression of TRIP8b(1a-4)-HA with EGFP-HCN1 enhanced expression of the channel in the surface membrane of CA1 neuron apical dendrites. However, the normal targeting of the channel to the distal dendrites was perturbed as HCN1 was present uniformly throughout the somatodendritic axis.

In our present experiments, we confirmed that overexpression of TRIP8b(1a-4)-HA enhanced expression and caused mislocalization of EGFP-HCN1 as previously described (Figure 8A, right;

compare to Figure 4A). In addition, by staining for the HA tag, we found that overexpressed TRIP8b(1a-4)-HA was present in a uniform dendritic distribution similar to that of EGFP-HCN1 (Figure 8A, left), in contrast to the distal dendritic localization of endogenous TRIP8b(1a-4) (see Figure 7A). Although overexpressed TRIP8b(1a-4)-HA fails to form a dendritic gradient, the fact that HCN1 is consistently colocalized with TRIP8b(1a-4), either under physiological conditions when both are targeted to distal dendrites or when TRIP8b(1a-4)-HA is overexpressed and both are present in a uniform distribution, suggests that TRIP8b(1a-4) is a key isoform that helps direct channel localization.

The above hypothesis is supported by the contrasting action of overexpressed TRIP8b(1a)-HA. When coexpressed with EGFP-HCN1, TRIP8b(1a)-HA was detected in an even distribution throughout CA1 pyramidal neurons (Figure 8B, left), similar to the localization of TRIP8b(1a-4)-HA. However, unlike with TRIP8b(1a-4)-HA, the dendritic expression of EGFP-HCN1 was unaltered by TRIP8b(1a)-HA, with the channel displaying a normal localization in CA1 distal dendrites (Figure 8B, right). The lack of change in EGFP-HCN1 dendritic targeting is consistent with the view that TRIP8b(1a) may act preferentially in axons.

Effects of Overexpression of HA-Tagged TRIP8b(1a-4) and TRIP8b(1a) on EGFP-HCN1 Trafficking in Axons of CA1 Pyramidal Neurons

To test directly the idea that TRIP8b(1a) prevents HCN1 mislocalization in CA1 pyramidal neuron axons, we examined the effects of overexpressing HA-tagged TRIP8b(1a) on axonal EGFP-HCN1. Although endogenous levels of HCN1 in CA1 pyramidal neuron axons are normally very low (see Lorincz et al., 2002; Notomi and Shigemoto, 2004), a strong fluorescence signal for overexpressed EGFP-HCN1 was observed in CA1 axonal fibers running through SO and alveus of the hippocampus (Figures 9A–9C). Perhaps the clearest evidence that EGFP-HCN1 was present in CA1 axons comes from our finding of a strong fluorescence signal in SO of CA1 and subiculum in the hemisphere contralateral to that where virus was injected

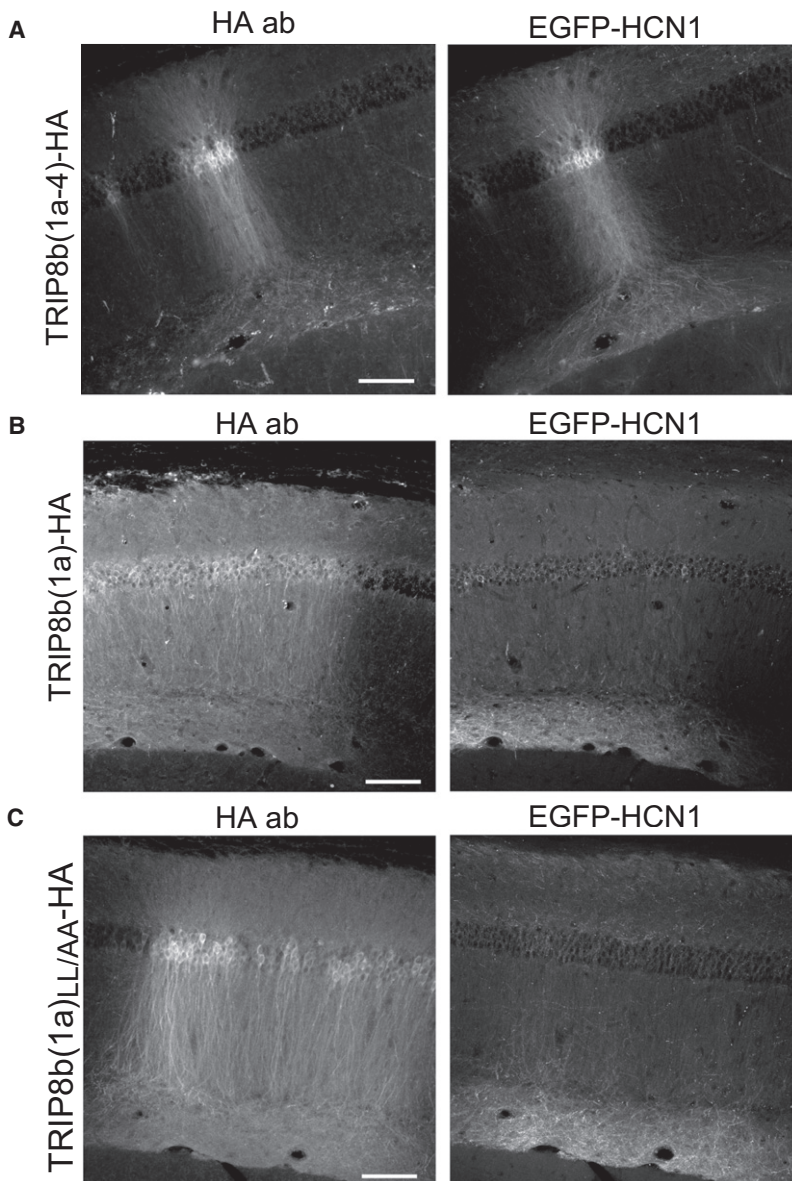


Figure 8. Overexpression of TRIP8b(1a-4), but Not TRIP8b(1a), Alters the Dendritic Expression Pattern of EGFP-HCN1

(A) CA1 region of hippocampus of HCN1 knockout mouse infected with independent viruses expressing HA-tagged TRIP8b(1a-4) and EGFP-HCN1. Left column. Immunofluorescence from anti-HA antibody, reflecting location of expressed TRIP8b(1a-4). Right column, EGFP-HCN1 fluorescence. Note how EGFP-HCN1 expression pattern mirrored that of TRIP8b(1a-4)-HA.

(B) Localization of virally expressed HA-tagged TRIP8b(1a) and coexpressed EGFP-HCN1.

(C) Localization of mutant TRIP8b(1a)_{LL/AA}-HA and coexpressed EGFP-HCN1. The scale bars represent 100 μ m.

Downregulation of HCN1 surface expression by TRIP8b(1a) in *Xenopus* oocytes is dependent on the presence of a dileucine adaptor protein trafficking motif in the control of axonal expression of HCN1 (Bonifacino and Traub, 2003) in the N-terminal domain of the TRIP8b protein (Santoro et al., 2009). To examine the importance of this motif we coexpressed EGFP-HCN1 with TRIP8b(1a)_{LL/AA}-HA, whose dileucine residues were substituted with alanine (L18A/L19A, see Santoro et al., 2009). Unlike the wild-type protein, TRIP8b(1a)_{LL/AA}-HA failed to prevent the mislocalization of EGFP-HCN1 in axons in both contralateral (Figure 9G) and ipsilateral hippocampus (Figure 8C), even though the mutant protein was expressed at high levels. These results strongly support the view that TRIP8b(1a) exerts a highly specific action to prevent HCN1 mislocalization in axons through a direct interaction with the channel and the likely recruitment of adaptor protein complexes.

DISCUSSION

Our results demonstrate that TRIP8b splice isoforms are necessary for the proper trafficking of HCN1 channels to the surface membrane of CA1 pyramidal neurons and for the proper targeting

(Figures 9A and 9B), sites where commissural CA1 axons are known to project (van Groen and Wyss, 1990).

Strikingly, coexpression of TRIP8b(1a)-HA with EGFP-HCN1 eliminated channel fluorescence in axon fibers in both contralateral (Figure 9F) and ipsilateral hippocampus (Figure 8B). This effect represents a local action to downregulate channel expression in axons because TRIP8b(1a)-HA caused no change in the dendritic expression of HCN1 (Figure 8B). Moreover the effect is isoform-specific as TRIP8b(1a-4)-HA had no effect on axonal expression of EGFP-HCN1 (Figure 9E). Further confirmation of the specificity of action of TRIP8b(1a) comes from our finding that TRIP8b(1a)-HA caused no change in the dendritic or axonal expression of EGFP-HCN1 _{Δ SNL} (Figure S7), whose membrane expression also cannot be downregulated by TRIP8b(1a) in *Xenopus* oocytes (Santoro et al., 2011; see Discussion).

of the channels to the distal dendritic compartment. Furthermore, of the more than ten TRIP8b isoforms present in brain, TRIP8b(1a) and TRIP8b(1a-4) appear to be most important for proper HCN1 localization in hippocampal CA1 pyramidal neurons. In particular, we suggest that TRIP8b(1a) largely prevents HCN1 misexpression in axons whereas TRIP8b(1a-4) enhances channel surface expression and ensures proper dendritic targeting.

Effect of General Knockdown of HCN1 Interaction with All TRIPb Isoforms

Lewis et al. (2009) previously reported that the reduction of all TRIP8b isoforms with siRNA suppresses HCN1 membrane expression and Ih in hippocampal neurons in dissociated cell culture. In addition to confirming these in vitro results, we

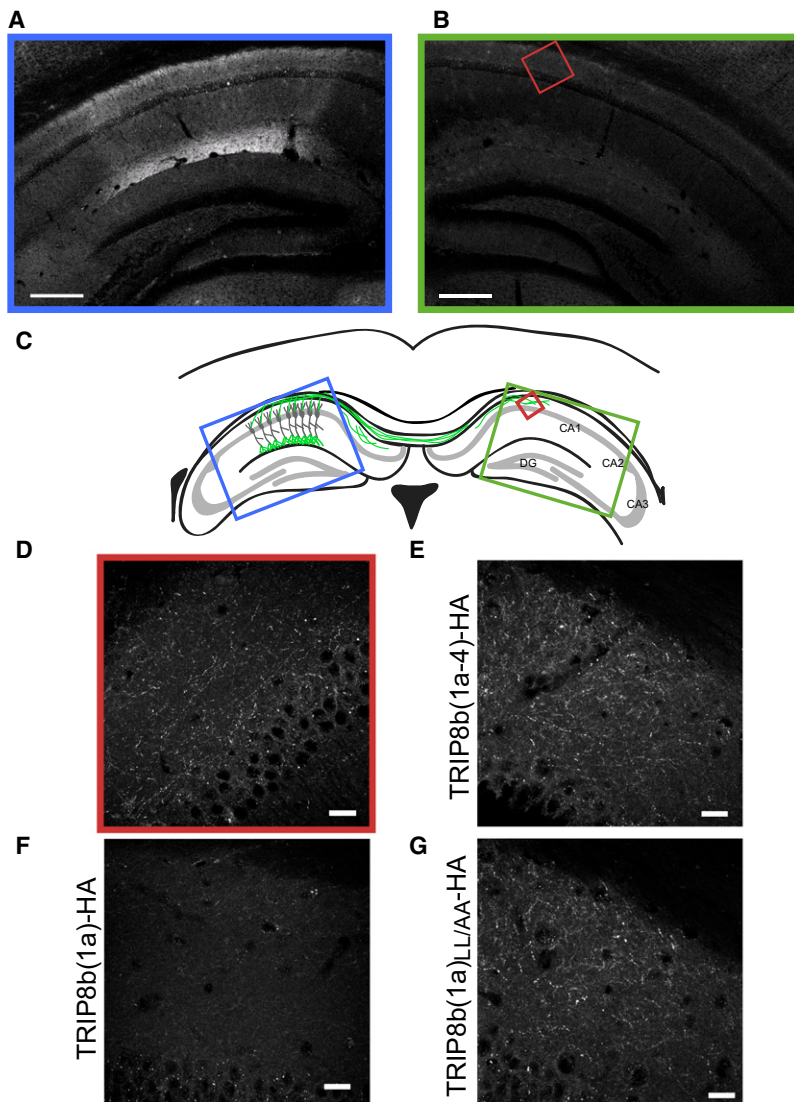


Figure 9. TRIP8b(1a) Downregulates Expression of EGFP-HCN1 in Axons

(A) Low magnification image of EGFP-HCN1 fluorescence from hippocampus of HCN1 KO mouse infected with independent TRIP8b(1a)-HA and EGFP-HCN1 viral vectors.

(B) Fluorescence image from uninjected contralateral hippocampus from same mouse. The scale bars represent 500 μm .

(C) Diagram illustrating the distal dendritic expression pattern of infected neurons at injection site and the location of axonal fibers in the contralateral hippocampus. The blue, green and red boxes correspond to the regions shown in (A), (B), and (D).

(D) Higher-magnification image of EGFP-HCN1 labeled axonal fibers in the contralateral hippocampus. The scale bar represents 20 μm .

(E–G) Similar experiment as in (A)–(D), except EGFP-HCN1 is coexpressed with TRIP8b(1a-4)-HA (E), TRIP8b(1a)-HA (F), or TRIP8b(1a)_{LL/AA}-HA (G). Note how TRIP8b(1a)-HA selectively downregulates EGFP-HCN1 in axons. The scale bar represents 20 μm .

Role of Different TRIP8b Isoforms in Regulating HCN1 Expression and Dendritic Localization

The task of defining the importance of individual TRIP8b splice forms in the surface expression and targeting of HCN1 to its proper neuronal compartments was greatly simplified by the availability of a mouse line, *Pex51^{tm1(KOMP)Vlcg}*, in which TRIP8b exons 1b and 2 were selectively deleted by homologous recombination. Remarkably, despite the loss of all but three of the more than ten TRIP8b splice forms normally present in the brain, the dendritic staining pattern of HCN1 was unaltered in CA1 neurons in the mutant mice. A comparison of TRIP8b expression in wild-type and KO mice further revealed that TRIP8b isoforms containing exons 1b or 2 are normally present predominantly in small CNPase-positive oligodendro-

cytes. The functional role of TRIP8b in these cells, and whether this role depends on an interaction with HCN2 channels present in oligodendrocytes, is unknown (Notomi and Shigemoto, 2004).

The data with the TRIP8b 1b/2 knockout mice strongly suggest that TRIP8b(1a-4) is a key isoform important in the establishment of the HCN1 dendritic gradient in CA1 pyramidal neurons. Thus, of TRIP8b(1a), TRIP8b(1a-4), and TRIP8b(1a-3-4), the three isoforms expressed in the knockout mice, TRIP8b(1a-3-4) is unlikely to be important as it is present at very low levels in brain (Santoro et al., 2009) and is not detected in hippocampus (Lewis et al., 2009). Because HCN1 dendritic targeting was unperturbed in the KO mouse but was disrupted when all TRIP8b isoforms were downregulated with siRNA (or when their interaction with HCN1 was inhibited in the HCN1_{ΔSNL} mutant), we conclude that either TRIP8b(1a-4) or TRIP8b(1a) must be necessary and sufficient for HCN1 to be properly localized to CA1 distal dendrites. Furthermore, as TRIP8b(1a) immunostaining

found that downregulation of TRIP8b in vivo inhibited HCN1 membrane expression and Ih in CA1 neurons. In particular, we observed a marked decrease in HCN1 expression in CA1 distal dendrites. Our results with in vivo siRNA knockdown thus provide clear evidence that TRIP8b is necessary for the proper expression and localization of HCN1 in CA1 neuronal compartments.

This conclusion is supported by our finding that an HCN1 truncation mutant lacking its C-terminal TRIP8b interaction peptide, HCN1_{ΔSNL}, which has a decreased affinity for TRIP8b, failed to localize to the CA1 distal dendrites. As the mutant channel was strongly expressed in the surface membrane throughout the somatodendritic compartment in a fairly uniform manner, we further conclude that HCN1 surface expression and dendritic targeting are dissociable functions of TRIP8b that are differentially sensitive to alterations in its biochemical interactions with HCN1 (see below).

was largely limited to axons, TRIP8b(1a-4) appears the most likely isoform required for dendritic targeting of HCN1. This view is supported by our finding that TRIP8b(1a-4) was concentrated and colocalized with HCN1 in the distal dendrites of CA1 neurons, in both wild-type and TRIP8b 1b/2 KO mice, and by previous results that overexpression of TRIP8b(1a-4) markedly enhances the surface expression of HCN1 in heterologous cells and CA1 pyramidal neurons (Santoro et al., 2009).

At first glance, our observation that HCN1 $_{\Delta\text{SNL}}$, which has a reduced binding affinity for all TRIP8b isoforms, was strongly expressed in the surface membrane of CA1 neurons seems at odds with the siRNA findings that TRIP8b in general was required for efficient trafficking of HCN1 to the surface membrane. However, TRIP8b and HCN1 have been recently found to interact at two distinct sites, only one of which involves the SNL sequence (Lewis et al., 2009; Santoro et al., 2011). In addition, our laboratory recently reported that TRIP8b(1a-4) retains its full functional ability to upregulate surface expression of the HCN1 $_{\Delta\text{SNL}}$ mutant channel when heterologously expressed in *Xenopus* oocytes. Thus, the residual interaction of TRIP8b(1a-4) with the mutant HCN1 channel is likely to account for its strong surface expression.

The ability of TRIP8b(1a-4) to upregulate surface membrane expression of HCN1 $_{\Delta\text{SNL}}$ raises the question as to why this interaction failed to localize properly the mutant channel to the CA1 distal dendrites. One explanation is that dendritic targeting and channel surface expression depend on distinct interactions of HCN1 with TRIP8b(1a-4) that are differentially sensitive to the loss of the SNL binding site. Alternatively, proper dendritic localization may require the cooperative interaction of TRIP8b(1a-4) with TRIP8b(1a), whose action to downregulate HCN1 surface expression in heterologous expression systems is eliminated upon deletion of the SNL tripeptide (Santoro et al., 2011).

A second result seemingly at odds with the hypothesis that TRIP8b(1a-4) specifies the dendritic gradient of HCN1 is that exogenously expressed TRIP8b(1a-4)-HA did not localize to distal CA1 dendrites but showed a relatively uniform expression throughout the somatodendritic compartment. We suggest that TRIP8b(1a-4) must interact with a separate trafficking element, possibly another protein or mRNA targeting motif, that is in limited supply. As a result, there may have been an insufficient amount of this factor to ensure proper dendritic targeting of TRIP8b(1a-4)-HA when it was overexpressed. Nonetheless, our finding that HCN1 expression matches that of TRIP8b(1a-4), both under physiological conditions when the two proteins are present in a dendritic gradient and during overexpression when both proteins are present in a uniform distribution, implies that the high concentration of endogenous TRIP8b(1a-4) in the distal dendrites of CA1 neurons should be sufficient to localize HCN1 channels at this site under physiological conditions.

Comparison of HCN1 Dendritic Targeting with Polarized Trafficking of Other Ion Channels

It is of interest to consider our findings on the role of TRIP8b isoforms in the trafficking of HCN1 in the context of previous results on the trafficking of other neuronal membrane proteins to different polarized neuronal compartments. Four distinct mechanisms have been reported (Arnold, 2009): (1) Some proteins are

present in transport vesicles that are directly targeted to the proper compartment. (2) Other proteins are shipped indiscriminately to all neuronal compartments, but then removed by endocytosis from inappropriate regions. (3) Still other proteins are also transported indiscriminately, but the transport vesicles only dock in the appropriate compartment. (4) Finally some proteins are targeted through transcytosis, in which the protein is first expressed in one compartment from which it is removed by endocytosis and then shipped to the appropriate locale through recycling endosomes (Lisiecka et al., 2009).

With respect to these four mechanisms, perhaps the simplest view is that TRIP8b(1a-4) promotes HCN1 distal dendritic targeting through mechanism 1 whereas TRIP8b(1a) prevents axonal mislocalization through mechanism 2. However, the two isoforms might also act sequentially through transcytosis (mechanism 4). This latter mechanism could explain why HCN1 $_{\Delta\text{SNL}}$, whose SNL truncation prevents its downregulation by TRIP8b(1a), fails to be targeted to the distal dendrites despite its continued interaction with TRIP8b(1a-4) that enhances channel surface expression. Exploration of these possibilities will provide an ample challenge for future work.

Functional Role and Dynamic Regulation of Dendritic HCN1 Channels in Hippocampal Pyramidal Neurons

By comparing the electrophysiological properties of CA1 neurons from HCN1 knockout mice that have been rescued with either full-length EGFP-HCN1 or EGFP-HCN1 $_{\Delta\text{SNL}}$, our experiments reveal how the proper targeting of HCN1 to its dendritic locale is required for the normal processing of information through the hippocampal circuit by CA1 neuron dendrites. Thus, we found that the preferential targeting of full-length HCN1 to the distal dendrites is required for the selective inhibitory action of this channel on the integration of distal PP EPSPs relative to more proximal SC EPSPs (Nolan et al., 2004). This selective effect helps ensure that the distal PP EPSPs will have a relatively weak influence at the CA1 neuron soma, relative to the proximal SC EPSPs. In contrast, we found that the mistargeting of EGFP-HCN1 $_{\Delta\text{SNL}}$ to proximal dendrites changes the normal balance of the two inputs, enhancing the contribution of the PP EPSPs while decreasing the contribution of the SC EPSPs.

The marked effects that the various TRIP8b isoforms exert on HCN1 surface levels also provide a potential molecular mechanism to explain the recent findings that the levels of Ih in neurons are not fixed but can be increased or decreased by different patterns of neural activity that induce synaptic plasticity (Brager and Johnston, 2007; Campanac et al., 2008; Fan et al., 2005). Alterations in TRIP8b-HCN1 interactions may also contribute to the maladaptive changes in HCN1 expression associated with seizures that is thought to contribute to the development of epilepsy (Brewster et al., 2002, 2005; Chen et al., 2001; Jung et al., 2007; Shah et al., 2004; Shin and Chetkovich, 2007), an effect that is, in part, due to a redistribution of HCN1 from the distal dendrites to the soma of CA1 neurons (Shin et al., 2008). Given the strong regulatory action of TRIP8b splice variants on the surface expression and compartmentalization of both native and exogenous HCN1 in vivo, it will be of interest to determine how changes in expression of specific TRIP8b isoforms plays

a role in these dynamic activity-dependent changes in Ih. Future studies examining the regulation of TRIP8b alternative splicing and posttranslational modifications by signaling cascades may further enhance our understanding of how this auxiliary subunit acts as a central regulator of Ih, thereby influencing the excitability and plasticity of the hippocampal circuit.

EXPERIMENTAL PROCEDURES

Lentivirus Expression

The lentiviral expression vector containing the CaMKII promoter, pFCK(0.4) GW was provided by Pavel Osten (Max Planck Institute, Heidelberg) (Dittgen et al., 2004). Subcloning and virus preparation were carried out essentially as described (Santoro et al., 2009; see also Supplemental Experimental Procedures). For in vivo delivery, virus was concentrated to 10^8 IU/ml in sterile saline and stereotactically injected into the hippocampal CA1 region of adult mice (aged 3–9 months). HCN1 knockout animals (genotype HCN1^{-/-}) were generated and bred as described (Nolan et al., 2003). For all siRNA and EGFP-HCN1_{ΔSNL} experiments, at least four animals were bilaterally injected for each experimental condition, with eight to ten injection sites analyzed. For all experiments investigating the interaction between EGFP-HCN1 and TRIP8b(1a-4) or TRIP8b(1a-4)-HA, 8 mice were unilaterally injected for each experimental condition, with eight injection sites analyzed.

Immunohistochemistry

Animals were perfused with ice-cold 1 × PBS followed by 4% paraformaldehyde in 1 × PBS; 50 μm slices were cut with a vibratome, and permeabilized in PBS+0.2% Triton, followed by incubation in blocking solution (PBS+0.2% Triton + 3% normal goat serum). For staining with the TRIP8b(1a) antibody, antibody retrieval was performed by incubating slices for 30 min in 10 mM sodium citrate at 80°C before blocking. Primary antibody incubation was carried out in blocking solution overnight at 4°C. For a complete list of antibodies used see Supplemental Experimental Procedures. Slices were mounted with Immuno-gold (Invitrogen), and fluorescence imaging performed on inverted laser scanning confocal microscopes (BioRad MRC 1000, Olympus FV1000, Zeiss LSM 700). For immunohistochemistry with Pex5^{tm1(KOMP)Vlcg} animals, two aged-matched pairs of Trip8b 1b/2 and control littermates were examined. All images were analyzed with ImageJ (NIH) and IGORPro software (Wavemetrics).

siRNA Knockdown

siRNA target sequences were selected using the GenScript and Ambion algorithms, and dsDNA oligonucleotides cloned into the pLLhS lentivirus vector (Nakagawa et al., 2004) under control of the U6 promoter. The pLLhS vector also expressed EGFP under the control of the synapsin promoter. siRNA efficacy was assayed by western blot analysis from cultured neuronal extracts; one TRIP8b siRNA construct greatly reduced the levels of TRIP8b protein (Figure 1) compared with control siRNA. This TRIP8b- siRNA targeted nucleotide positions 1419–1439 in the TRIP8b(1b-2) isoform cDNA sequence (5'-CCA CCTGAGTGGAGAGTCAA-3') in constant exon 14 (Santoro et al., 2009). The control siRNA construct was similarly constructed, but encodes a scrambled target sequence. Histology and electrophysiology were performed two to 3 weeks after viral injection.

TRIP8b Exon 1b/2 Knockout Mouse

The Trip8b exon1b and 2 knockout mice were generated by the NIH KOMP mutagenesis project. Details of the mouse can be found at www.komp.org. In summary, Regeneron designed the targeting vector (project ID VG11153) used to generate the allele Pex5^{tm1(KOMP)Vlcg}. The lacZ coding sequence was inserted directly after the start codon in exon 1b, followed by a neomycin selection cassette flanked by loxP sites, replacing all of exons 1b and 2 (see Figure S3). Note that despite the presence of polyadenylation sites both following the lacZ as well as the neomycin coding sequences in the targeting cassette, alternate start sites still enabled translation of TRIP8b splice isoforms starting with exon 1a (see Figure 6A and Figure S2). The occurrence of read-through transcripts from exon 1a through the constant region of TRIP8b was verified through RT-PCR (data not shown).

Acute Hippocampal Slices and Electrophysiology

Lentivirus was stereotactically injected into the dorsal hippocampi of 5-week-old mice. Transverse hippocampal slices (400 μm) were prepared two weeks after viral injection. Animals were sacrificed in accordance to institutional IACUC standards. For solution composition and detailed methods see Supplemental Experimental Procedures. Virally infected neurons were identified by EGFP fluorescence. Following recordings of infected neurons, slices were fixed for 30 min in PFA and imaged to ensure that all dye-filled cells were also EGFP+ and that the dendritic structure of infected cells was normal. Series resistance was less than 15 MΩ; capacitance and series resistance were monitored and compensated throughout the experiments. Recordings were performed at 32°C. All data was acquired with Pclamp software (Molecular Devices) and analyzed with IGORPro (wavemetrics).

SUPPLEMENTAL INFORMATION

Supplemental Information includes Supplemental Experimental Procedures and seven figures and can be found with this article online at [doi:10.1016/j.neuron.2011.03.023](https://doi.org/10.1016/j.neuron.2011.03.023).

ACKNOWLEDGMENTS

This work was supported by grants NS36658 and MH80745 from NIH, by fellowships from NIH F32NS064732 (R.P.), the Italian Academy for Advanced Studies in America (B.S.) and a Research Grant from the Epilepsy Foundation (B.S.). We gratefully acknowledge Terunaga Nakagawa and Morgan Sheng for providing the pLLhS and Pavel Osten for providing the pFCK(0.4)GW lentiviral vectors, and Frank Müller for generously providing the rat 7C3 monoclonal HCN1 antibody. We thank Ming-Kuei Jang and Thomas Yocum for preliminary experiments, Haiying Liu for technical assistance and Vivien Chevalyre for experimental advice.

Accepted: March 30, 2011

Published: May 11, 2011

REFERENCES

- Arnold, D.B. (2009). Actin and microtubule-based cytoskeletal cues direct polarized targeting of proteins in neurons. *Sci. Signal.* 2, pe49.
- Bonifacino, J.S., and Traub, L.M. (2003). Signals for sorting of transmembrane proteins to endosomes and lysosomes. *Annu. Rev. Biochem.* 72, 395–447.
- Brager, D.H., and Johnston, D. (2007). Plasticity of intrinsic excitability during long-term depression is mediated through mGluR-dependent changes in Ih in hippocampal CA1 pyramidal neurons. *J. Neurosci.* 27, 13926–13937.
- Brewster, A., Bender, R.A., Chen, Y., Dube, C., Eghbal-Ahmadi, M., and Baram, T.Z. (2002). Developmental febrile seizures modulate hippocampal gene expression of hyperpolarization-activated channels in an isoform- and cell-specific manner. *J. Neurosci.* 22, 4591–4599.
- Brewster, A.L., Bernard, J.A., Gall, C.M., and Baram, T.Z. (2005). Formation of heteromeric hyperpolarization-activated cyclic nucleotide-gated (HCN) channels in the hippocampus is regulated by developmental seizures. *Neurobiol. Dis.* 19, 200–207.
- Campanac, E., Daoudal, G., Ankri, N., and Debanne, D. (2008). Downregulation of dendritic Ih in CA1 pyramidal neurons after LTP. *J. Neurosci.* 28, 8635–8643.
- Chen, K., Aradi, I., Thon, N., Eghbal-Ahmadi, M., Baram, T.Z., and Soltesz, I. (2001). Persistently modified h-channels after complex febrile seizures convert the seizure-induced enhancement of inhibition to hyperexcitability. *Nat. Med.* 7, 331–337.
- Dittgen, T., Nimmerjahn, A., Komai, S., Licznarski, P., Waters, J., Margrie, T.W., Helmchen, F., Denk, W., Brecht, M., and Osten, P. (2004). Lentivirus-based genetic manipulations of cortical neurons and their optical and electrophysiological monitoring in vivo. *Proc. Natl. Acad. Sci. USA* 101, 18206–18211.

- Fan, Y., Fricker, D., Brager, D.H., Chen, X., Lu, H.C., Chitwood, R.A., and Johnston, D. (2005). Activity-dependent decrease of excitability in rat hippocampal neurons through increases in I(h). *Nat. Neurosci.* *8*, 1542–1551.
- George, M.S., Abbott, L.F., and Siegelbaum, S.A. (2009). HCN hyperpolarization-activated cation channels inhibit EPSPs by interactions with M-type K(+) channels. *Nat. Neurosci.* *12*, 577–584.
- Jung, S., Jones, T.D., Lugo, J.N., Jr., Sheerin, A.H., Miller, J.W., D'Ambrosio, R., Anderson, A.E., and Poolos, N.P. (2007). Progressive dendritic HCN channelopathy during epileptogenesis in the rat pilocarpine model of epilepsy. *J. Neurosci.* *27*, 13012–13021.
- Lasiecka, Z.M., Yap, C.C., Vakulenko, M., and Winckler, B. (2009). Compartmentalizing the neuronal plasma membrane from axon initial segments to synapses. *Int. Rev. Cell Mol. Biol.* *272*, 303–389.
- Lewis, A.S., Schwartz, E., Chan, C.S., Noam, Y., Shin, M., Wadman, W.J., Surmeier, D.J., Baram, T.Z., Macdonald, R.L., and Chetkovich, D.M. (2009). Alternatively spliced isoforms of TRIP8b differentially control h channel trafficking and function. *J. Neurosci.* *29*, 6250–6265.
- Lorincz, A., Notomi, T., Tamas, G., Shigemoto, R., and Nusser, Z. (2002). Polarized and compartment-dependent distribution of HCN1 in pyramidal cell dendrites. *Nat. Neurosci.* *5*, 1185–1193.
- Magee, J.C. (1998). Dendritic hyperpolarization-activated currents modify the integrative properties of hippocampal CA1 pyramidal neurons. *J. Neurosci.* *18*, 7613–7624.
- Magee, J.C. (1999). Dendritic I_h normalizes temporal summation in hippocampal CA1 neurons. *Nat. Neurosci.* *2*, 508–514.
- Nakagawa, T., Futai, K., Lashuel, H.A., Lo, I., Okamoto, K., Walz, T., Hayashi, Y., and Sheng, M. (2004). Quaternary structure, protein dynamics, and synaptic function of SAP97 controlled by L27 domain interactions. *Neuron* *44*, 453–467.
- Nolan, M.F., Malleret, G., Lee, K.H., Gibbs, E., Dudman, J.T., Santoro, B., Yin, D., Thompson, R.F., Siegelbaum, S.A., Kandel, E.R., and Morozov, A. (2003). The hyperpolarization-activated HCN1 channel is important for motor learning and neuronal integration by cerebellar Purkinje cells. *Cell* *115*, 551–564.
- Nolan, M.F., Malleret, G., Dudman, J.T., Buhl, D.L., Santoro, B., Gibbs, E., Vronskaya, S., Buzsaki, G., Siegelbaum, S.A., Kandel, E.R., and Morozov, A. (2004). A behavioral role for dendritic integration: HCN1 channels constrain spatial memory and plasticity at inputs to distal dendrites of CA1 pyramidal neurons. *Cell* *119*, 719–732.
- Notomi, T., and Shigemoto, R. (2004). Immunohistochemical localization of I_h channel subunits, HCN1-4, in the rat brain. *J. Comp. Neurol.* *471*, 241–276.
- Santoro, B., Grant, S.G., Bartsch, D., and Kandel, E.R. (1997). Interactive cloning with the SH3 domain of N-src identifies a new brain specific ion channel protein, with homology to eag and cyclic nucleotide-gated channels. *Proc. Natl. Acad. Sci. USA* *94*, 14815–14820.
- Santoro, B., Wainger, B.J., and Siegelbaum, S.A. (2004). Regulation of HCN channel surface expression by a novel C-terminal protein-protein interaction. *J. Neurosci.* *24*, 10750–10762.
- Santoro, B., Piskorowski, R.A., Pian, P., Hu, L., Liu, H., and Siegelbaum, S.A. (2009). TRIP8b splice variants form a family of auxiliary subunits that regulate gating and trafficking of HCN channels in the brain. *Neuron* *62*, 802–813.
- Santoro, B., Hu, L., Liu, H., Saponaro, A., Pian, P., Piskorowski, R., Moroni, A., and Siegelbaum, S. (2011). TRIP8b regulates HCN1 channel trafficking and gating through two distinct C-terminal interaction sites. *J. Neurosci.* *31*, 4074–4088.
- Shah, M.M., Anderson, A.E., Leung, V., Lin, X., and Johnston, D. (2004). Seizure-induced plasticity of h channels in entorhinal cortical layer III pyramidal neurons. *Neuron* *44*, 495–508.
- Shin, M., and Chetkovich, D.M. (2007). Activity-dependent regulation of h channel distribution in hippocampal CA1 pyramidal neurons. *J. Biol. Chem.* *282*, 33168–33180.
- Shin, M., Brager, D., Jaramillo, T.C., Johnston, D., and Chetkovich, D.M. (2008). Mislocalization of h channel subunits underlies h channelopathy in temporal lobe epilepsy. *Neurobiol. Dis.* *32*, 26–36.
- Tsay, D., Dudman, J.T., and Siegelbaum, S.A. (2007). HCN1 channels constrain synaptically evoked Ca²⁺ spikes in distal dendrites of CA1 pyramidal neurons. *Neuron* *56*, 1076–1089.
- van Groen, T., and Wyss, J.M. (1990). Extrinsic projections from area CA1 of the rat hippocampus: Olfactory, cortical, subcortical, and bilateral hippocampal formation projections. *J. Comp. Neurol.* *302*, 515–528.
- Zolles, G., Wenzel, D., Bildl, W., Schulte, U., Hofmann, A., Muller, C.S., Thumfart, J.O., Vlachos, A., Deller, T., Pfeifer, A., et al. (2009). Association with the auxiliary subunit PEX5R/Trip8b controls responsiveness of HCN channels to cAMP and adrenergic stimulation. *Neuron* *62*, 814–825.